

REPORT DOCUMENTATION PAGE			Form Approved OMB No. 0704-0188	
Public reporting burden for this collection of information is estimated to average 1 hour per response, including the time for reviewing instructions, searching existing data sources, gathering and maintaining the data needed, and completing and reviewing the collection of information. Send comments regarding this burden estimate or any other aspect of this collection of information, including suggestions for reducing this burden, to Washington Headquarters Services, Directorate for Information Operations and Reports, 1215 Jefferson Davis Highway, Suite 1204, Arlington, VA 22202-4302, and to the Office of Management and Budget, Paperwork Reduction Project (0704-0188), Washington, DC 20503.				
1. AGENCY USE ONLY (Leave Blank)	2. REPORT DATE March 31, 2007	3. REPORT TYPE AND DATES COVERED Final Technical Report, June 2001-November 30, 2006.		
4. TITLE AND SUBTITLE Basic Research Leading to Compact, Portable Pulsed Power FY'01 MURI Consortium		5. FUNDING NUMBERS F496200110354		
6. AUTHORS Edl Schamiloglu, Karl Schoenbach and Robert Vidmari				
7. PERFORMING ORGANIZATION NAME(S) AND ADDRESS(ES) University of New Mexico Department of Electrical and Computer Engineering MSC01 1100 Albuquerque, NM 87131-00-1		8. PERFORMING ORGANIZATION REPORT NUMBER		
9. SPONSORING / MONITORING AGENCY NAME(S) AND ADDRESS(ES) AFOSR/NE 875 North Randolph St., Suite 325 Arlington, VA 22203-1977 Dr. Robert J. Barker, PM		10. SPONSORING / MONITORING AGENCY REPORT NUMBER AFRL-SR-AR-TR-07-0119		
11. SUPPLEMENTARY NOTES				
12a. DISTRIBUTION / AVAILABILITY STATEMENT Unlimited <i>Distribution Statement A: unlimited</i>		12b. DISTRIBUTION CODE AFOSR/NE		
13. ABSTRACT (Maximum 200 words) Pulsed power is a technology that is suited to drive electrical loads requiring very large power pulses in short bursts (high-peak power). Certain applications require technology that can be deployed in small spaces under stressful environments, e.g., on a ship, vehicle, or aircraft. In 2001, the U.S. Department of Defense (DoD) launched a long-range (five-year) Multidisciplinary University Research Initiative (MURI) to study fundamental issues for compact pulsed power. This research program endeavored to: 1) introduce new materials for use in pulsed power systems; 2) examine alternative topologies for compact pulse generation; 3) study pulsed power switches, including pseudospark switches; and 4) investigate the basic physics related to the generation of pulsed power, such as the behavior of liquid dielectrics under intense electric field conditions. This final technical report reviews the advances put forth by the researchers in this consortium and will assess the potential impact for future development of compact pulsed power systems. The progress made over the final 18 months of the program is emphasized. The key achievements of this research program are: i) liquid breakdown has been extensively diagnosed and new models to explain the observed behavior have been proposed; ii) dielectric breakdown under pulsed power conditions was observed to occur at a lower threshold (about 75%) compared with quasi-DC breakdown for a wide range of materials ranging from common Mylar to complicated high dielectric nanopowder-impregnated epoxy resin – a new model to explain this behavior for nanocrystalline TiO2 has been proposed; fundamental limitations in achieving compact, folded planar Blumlein transmission lines have been identified; the investigation of a 100-to-1 impedance ratio exponential line demonstrated an approach to maintaining coherent phase fronts at the wide low-impedance end of an exponential line – fundamental limitations to this approach, as well as the use of turbulent capillary flow for mitigating thermal loading were identified.				
14. SUBJECT TERMS Pulsed power, compact pulsed power, Blumlein, electromagnetic modeling, high pressure switches, liquid breakdown, dielectric breakdown, thermal management.		15. NUMBER OF PAGES 34		16. PRICE CODE
17. SECURITY CLASSIFICATION OF REPORT Unclassified	18. SECURITY CLASSIFICATION OF THIS PAGE Unclassified	19. SECURITY CLASSIFICATION OF ABSTRACT Unclassified	20. LIMITATION OF ABSTRACT None	



**The University of New Mexico
Pulsed Power, Beams and Microwaves Laboratory,
Department of Electrical & Computer Engineering**

**FY'01 MURI Consortium:
Basic Research Leading to Compact, Portable Pulsed Power
Final Technical Report
1 June 2001 – 30 November 2006**

31 March 2007

Submitted by:

Edl Schamiloglu — PI
Gardner-Zemke Professor,
Department of Electrical
and Computer
Engineering
University of New Mexico
Albuquerque, NM 87131
Tel. (505) 277-4423
Fax: (505) 277-1439
edl@ece.unm.edu

Karl H. Schoenbach
Eminent Scholar, Batten
Endowed Chair in
Bioelectric Engineering,
Frank Reidy Research
Center for Bioelectronics
Old Dominion University
830 Southampton Avenue,
Suite 5100
Norfolk, VA 23510

Robert Vidmar
Research Professor,
Physics Department,
University Of Nevada,
Reno
Physics Room 206, 5625
Fox Ave, Reno, NV 89506



20070417194

TABLE OF CONTENTS

EXECUTIVE SUMMARY	4
UNM - LIST OF ACHIEVEMENTS	5
Research in Support of the Development of a Compact Blumlein Pulser Test Bed.....	5
Background:.....	5
Accomplishments:.....	5
Liquid Breakdown Studies in Support of Task 1.....	14
High Dielectric Constant Ceramics for Use in Blumlein Transmission Lines	14
UNM PERSONNEL.....	16
UNM PUBLICATIONS.....	17
UNM RECOGNITION.....	19
UNM - NEW DISCOVERIES, INVENTIONS, PATENTS.....	19
ODU INTRODUCTION.....	21
ODU - LIST OF ACHIEVEMENTS	21
High repetition-rate, compact, nanosecond pulse generator	22
Electrical Triggering of Water Switches.....	23
ODU PUBLICATIONS	25
UNR ABSTRACT	26
UNR INTRODUCTION.....	28
UNR - LIST OF ACHIEVEMENTS	29
A. Exponential Transmission Line Modeling	29
B. RF Power Termination	29
UNR - SUMMARY OF RESULTS	31
A. Limitations in Implementation of Exponential Line Theory	31
B. Results from an Exponential Line with a 100-to-1 Impedance Ratio	31
C. Utilization of RF Chip Termination Resistors	32
UNR PERSONNEL	33
UNR PUBLICATIONS	33
UNR REFERENCES.....	34

EXECUTIVE SUMMARY

Pulsed power is a technology that is well-suited to driving electrical loads requiring very large power pulses in short bursts (high-peak power). Certain applications require technology that can be deployed in small spaces under stressful environments, *e.g.*, on a ship, vehicle, or aircraft. In 2001, the U.S. Department of Defense (DoD) launched a five-year Multidisciplinary University Research Initiative (MURI) to study fundamental issues for compact pulsed power. This research program endeavored to: 1) introduce new materials for use in pulsed power systems; 2) examine alternative topologies for compact pulse generation; 3) study pulsed power switches, including pseudospark switches; and 4) investigate the basic physics related to the generation of pulsed power, such as the behavior of liquid dielectrics under intense electric field conditions. Furthermore, the integration of all of these building blocks is impacted by system architecture (how things are put together). The main application for which this MURI program received its motivation from is intense beam-driven sources of high power microwaves (HPM). (A sister consortium led by USC also contributed to this overall program.)

After the three-year mid-point review the DoD advisory panel recommended that the Compact Pulsed Power MURI teams focus their efforts on liquid breakdown as the main technical challenge. Other research topics continued in parallel, albeit with diminished emphasis.

This final technical report summarizes the critical advances put forth by the researchers in this consortium. The emphasis of this report is on the last 18 months of the program. Technical summaries of earlier efforts, as well as a listing of publications, can be found in the yearly annual reports that were submitted. For ease of exposition, the report is organized by the participating universities. Old Dominion University was the lead on the liquid breakdown studies.

The key achievements of this research program are: i) liquid breakdown (for water and propylene carbonate) has been extensively diagnosed and new models to explain the observed behavior have been proposed; ii) dielectric breakdown under pulsed power conditions was observed to occur at a lower threshold (about 75%) compared with quasi-DC breakdown for a wide range of materials ranging from common Mylar to complicated high dielectric nanopowder-impregnated epoxy resin – a new model to explain this behavior for nanocrystalline TiO_2 has been proposed; fundamental limitations in achieving compact, folded planar Blumlein transmission lines have been identified; the investigation of a 100-to-1 impedance ratio exponential line demonstrated the feasibility of an approach to maintaining coherent phase fronts at the wide low-impedance end of an exponential line – fundamental limitations to this approach, as well as the use of turbulent capillary flow for mitigating thermal loading were identified.

UNM - LIST OF ACHIEVEMENTS

Research in Support of the Development of a Compact Blumlein Pulser Test Bed

Background:

The research described in this subsection was to support the development of a 600 kV, 50 ns, 5 Ω compact pulse-shaping drive that would be significantly lighter than coaxial water transmission line systems. Whereas researchers in the past have studied stacked-Blumlein arrangements using coaxial cable,¹ it is anticipated that a higher energy density (and therefore more compact) system can be achieved using a folded stripline geometry. Studies by Alexander *et al.* at Sandia National Laboratories² demonstrated that propylene carbonate-impregnated Kapton™ sheets are attractive for constructing high average field striplines that can be folded into a compact geometry. Such a compact source can be used to drive low impedance HPM sources (such as a Vircator, MILO, or relativistic magnetron) on a portable platform.

Accomplishments:

The initial Blumlein transmission line configuration that is being studied is the system described earlier.² The pulser that was used to charge the pulse-shaping section is a 6-stage bipolar charged Marx system. The capacitors in the Marx are 0.2 μ F, 100 kV cans and the switches are Maxwell™ midplane-triggered pancake spark gaps. The pulse shaping section comprises the Blumlein transmission line and its switch (triggered rail gap).

The Blumlein transmission line section utilized 10" wide copper strips with 2" Kapton™ margins in a 48" line that was folded into a 15" long unit. The dimensions were selected to achieve the design line impedance Z utilizing

$$Z \approx \frac{377 * d}{w * \sqrt{\epsilon_r}} \Omega, \quad (1)$$

where d is the thickness of the dielectric medium, w is the width of the line (assuming $d/w < 0.1$), and ϵ_r is the dielectric constant. The parameters utilized yield an impedance of 5 Ω .

Electromagnetic Modeling in Support of This Task:

The approach at UNM was to first model the actual folded Blumlein configuration electromagnetically. In Fig. 1 we present the results of an HFSS™ (Agilent/Ansoft)

¹ See, for example, I.C. Somerville, S.J. MacGregor, and O. Farish, "An Efficient Stacked-Blumlein HV Pulse Generator, *Meas. Sci. Technol.* 1, 865 (1990) and references therein.

² J.A. Alexander, S. Shope, R. Pate, L. Rinehart, J. Jojola, M. Ruebush, W. Crowe, J. Lundstrom, T. Smith, D. Zagar, and K. Prestwich, "Plastic Laminate Pulsed Power Development," *Proceedings, Society of Automotive Engineers*, Paper 00PSC-113 (San Diego, CA, October, 2000).

calculation to explore the electric field distribution between the center and outer conductors of the Blumlein configuration. In this configuration a voltage waveform is launched between the top and center conductors. A portion of the waveform is transmitted and propagates between the center conductor and the bottom conductor. A portion of the waveform reflects back upstream in the top section. Finally, after a double transit time, the full line charge voltage appears at the load (shown to be at the end of the line where the coordinate axes are defined in the sketch).

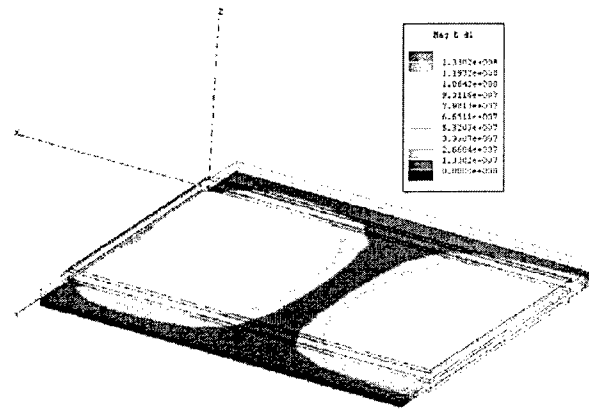


Figure 1. Calculation of voltage distribution at the load (defined by the position of the coordinate axes in the sketch). The red indicates full charge voltage at the load.

The importance of such calculations is to ultimately include the effects of resistivity grading at the outer ends of the line (where the dielectric and liquid interact) and to propose tailored dielectrics.

The research on this topic finally focused on using CST Microwave Studio as the simulation tool of choice. Two issues were studied: i) the effects that multi-switch excitation has on the response of a parallel-plate Blumlein line, and ii) the effects of using a multi-layer dielectric in a parallel-plate Blumlein pulse-forming line.

Effects of Multi-Switch Excitation

It is known that the use of multiple switches achieves faster rise time by reducing the overall inductance.³ Total inductance is inversely proportional to the number of switches in the system. In this work we examine where the practical limit to this is, *i.e.* what the number of switches is when no further change is observed if the number of switches is increased. However, in this work, we do not model the switch using its inductance, but rather by using the voltage transition produced by switch triggering. All the results here are produced using CST Microwave Studio™, a 3D-electromagnetic solver.

To better observe the effects of multi-switch excitation, we applied to a few model lines of

³ S.T. Pai and Q. Zhang, *Introduction to High Power Pulse Technology*, World Scientific, 1995.

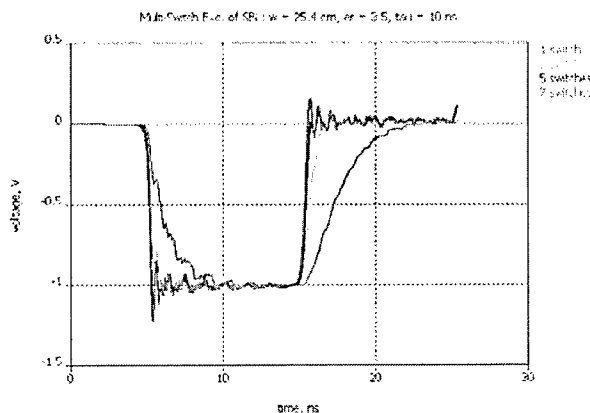
different widths. We compared the line response to a growing number of switches in each model in terms of the pulse width on the load, and maximum electric field. Following that, the pulse robustness against the imperfect triggering of the multi-switch system was shown (*i.e.*, a couple of delayed-triggering models). Ultimately, we test the use of smaller spacing between the switches near the edge of the line to see if that will further improve the responsiveness of the line.

Load Pulse Shapes

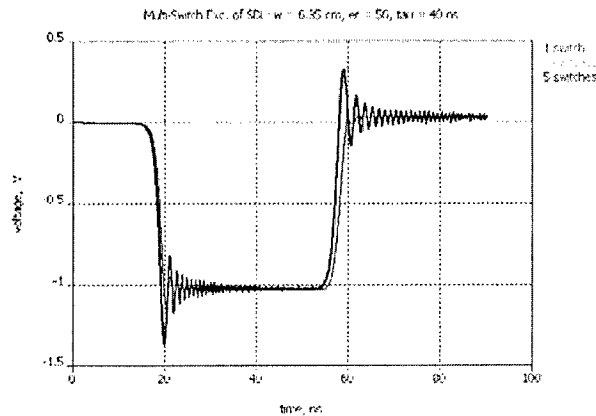
For this examination, we used four line widths: a) $w = 25.4$ cm, b) $w = 19.05$ cm, c) $w = 12.7$ cm, and d) $w = 6.35$ cm. It was estimated that case (a) can be tested for up to 7 switches, while cases (b) through (d) will use up to 5 switches. To have a symmetrical distribution of switches, odd numbers of them are used, as well as equal spacing between them, with one switch always placed in the center of the line width (later shown in Fig. 4a). Also, it was initially assumed that all the switches trigger at the same time.

Figure 2 shows a comparison of the pulses created by multiple switches for the above cases (a) and (d). The behavior of cases (b) and (c) is qualitatively and quantitatively in between these two cases.

The following observations can be drawn from these figures: use of a multi-switch excitation shortens the pulse, in general; the greater the number of switches, the shorter the pulse (this effect is stronger in a wider line); but, as the number of switches grows, the change in the pulse length is smaller and the pulse exhibits a growing ripple. At that point, the pulse length does not practically change with the increase in the number of switches, but the ripple does. The ripple is greater if the line is narrower. In addition, the pulse will be slightly shorter (*i.e.* the edges steeper) for a narrower line.



(a)



(b)

Figure 2. Blumlein response to a different number of switches for: a) $w = 25.4$ cm; b) $w = 6.35$ cm.

Our results qualitatively agree with the observations made about the effects of multiple switches in an experimental work.⁴ Both results show somewhat faster saturation than theoretical analysis would suggest. The theory states that the total inductance of a multi-switch excitation is approximately equal to $L = L_i/n$, where L_i is the inductance of a single switch, and n is the number of switches, assuming equal switches are utilized. Thus, the inductance should be steadily dropping as the number of switches increases (most noticeably for up to 8 switches), which can be verified by plotting the relative change of the total inductance with respect to a single-switch system. The results in Fig. 2 (and the cases (b) and (c) that are not shown) match that expectation, but saturate quite faster – almost after having 3 switches in the system. Therefore, these results suggest that, if a multi-switch system is used, there seems to be no advantage of using more than 3 switches in the system (using comparable line widths to these used in cases (b) to (d)).

Effects of Triggering Delay Between Switches

In the above simulations, we modeled all the switches to trigger at the same instant in time. That is an ideal situation to deal with, but a realistic system can exhibit a delay involved between the switches during the triggering process. Here, two cases are studied. In the first case, we assume that the switches trigger consecutively from the outermost switch of one end of the line towards the opposite outermost switch, and we refer to this case as a *single-sided delay*. For this case, we assign a constant delay of 0.3 ns. In the second case, we assume that the switch in the center triggers first, followed by the adjacent switches on each side towards the outermost switches. This case is referred to as *double-sided delay* and the delay time assigned to it is 0.3 ns as well.

⁴ J. Lehr, "High Power Water Switches for ZR at Sandia National Laboratories," [seminar talk], IEEE Albuquerque Chapter, January 20, 2005.

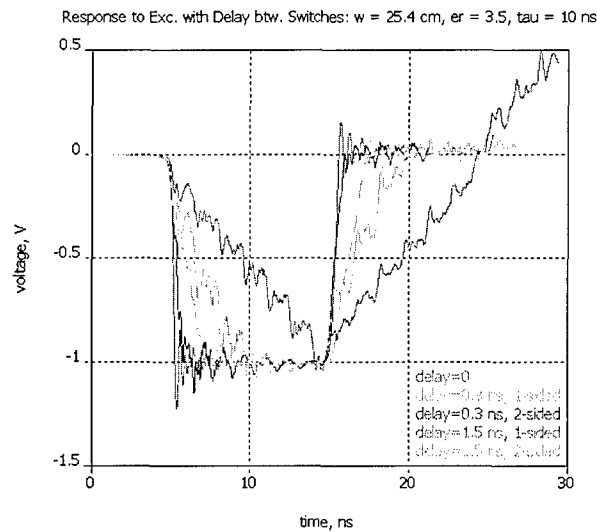


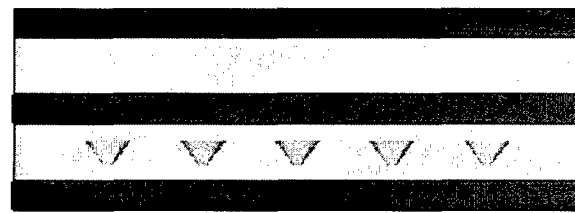
Figure 3. Output pulse after different triggering-delay patterns in the multi-switch excitation.

The results are shown in Fig. 3, compared to a no-delay case. For 0.3 ns-delay, the line response is robust against the triggering-synchronism imperfections of the multi-switch excitation system, especially for a 2-sided pattern. However, if a delay of 1.5 ns occurred, the response would still hold up for the 2-sided delay pattern, but it would be entirely corrupted for the 1-sided delay case. Overall, these cases give us a pattern and a range of switch-delay values for which the line can still produce a regular pulse.

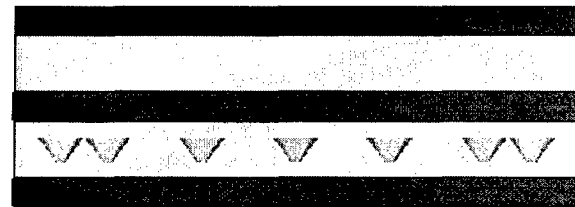
Unequal Spacing Between Switches

Since it was noted that the effects of a multi-switch system weaken with the growing number of switches, one can suspect that the switches in the central part have more influence in the multi-switch system. To improve that situation, one idea may be to use a higher density of the switches near the edges of the line.⁴ Therefore, we modified our original cases (a), and (d), each comprising their maximum number of switches, by adding switches on each side of the excitation system. Four of these configurations were tried, each with different spacing and switch position. If the original separation of the switches is denoted with s , these added switches have separations of $s/2$, $s/3$, and $s/4$.

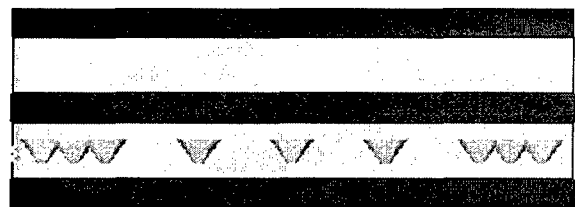
New test configurations in comparison with the “original” one are sketched in Fig. 4 for a 5-switch system. They are analogously set in the 7-switch system. These four test configurations should be sufficient if there is any advantage of using an increased switch density at the outer part of the line.



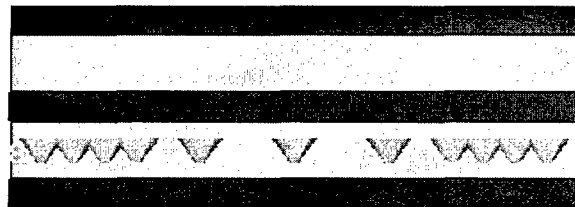
(a)



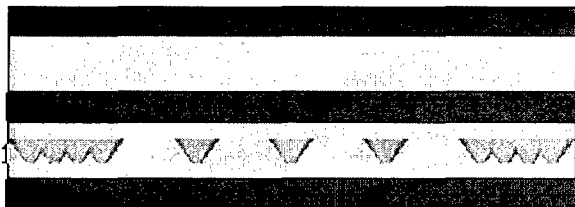
(b)



(c)



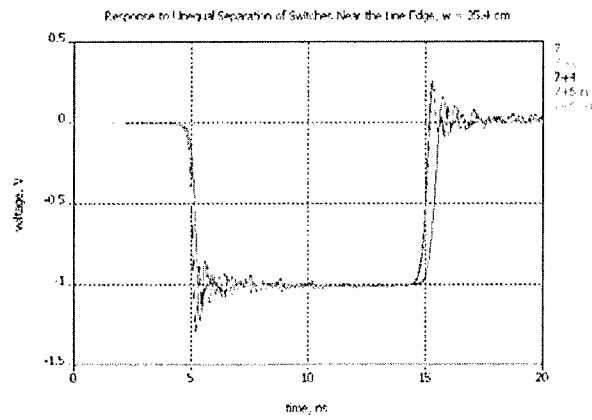
(d)



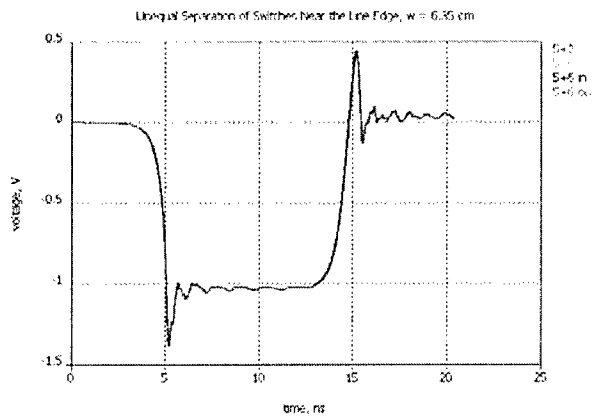
(e)

Figure 4. Configurations of a multi-switch system: a) equidistant; b) 1 switch added outwardly (on each side) at $s/2$ distance (called 5+2); c) 2 switches added at $s/3$ distance each (called 5+4); d) 3 switches added at $s/3$: 2 switches outwardly, and 1 switch inwardly (called 5+6 in); e) 3 switches added outwardly at $s/4$ each (called 5+6 out).

In addition, the configuration in Fig. 4d makes a more gradual transition from the original equidistant configuration by inserting one switch between the original switches 1 and 2.



(a)



(b)

Figure 5. Blumlein line response to adding more switches near the edge of the line for line width: a) 25.4 cm; b) 6.35 cm.

The result for the line cases (a), and (d) are shown in Fig. 5. In the case of the wider line, these additional switches did shorten the pulse a little (previously mentioned general rule applied), by affecting the falling edge of the pulse, but there is practically no difference in responses produced by the different configurations in Fig. 4. In the case of a narrow line in Fig. 5(b), these additional switch combinations showed no difference to the original 5-switch setting.

Effects of using a Multi-Layer Dielectric

The analyses were performed using the CST Microwave Studio software on a scaled down version of a straight, parallel-plate Blumlein line with the following parameters: the width $w = 1$ cm, the length $L = 3$ cm, the permittivity of the dielectric $\epsilon_r = 30$, the thickness of the dielectric slab $d = 0.762$ cm. The size was chosen to reduce the amount of computation time

required for a full scale model. The choice of 15 and 5 layers with this separation of electrodes provides good paradigms and “rounded” numbers for the thickness of each layer, which enables accurate modeling. Here we report the results from the 15-layer model.

The conductivity function was derived based on the following principle: minimum and maximum conductivity values were first and, depending on the actual number of layers used in the design, the remaining values of conductivity were then derived such that equal increments (steps) between the minimum and maximum value were obtained. The electric field (E-field, for short) inside the layers was recorded using a probe that was inserted in the vertical center of each layer at the edge of the line, where the maximum fields are reported to occur [10-12].

15-layer Model

This design comprises 15 equally thick layers of the layer thickness $d_l = d/15$. The conductivity (σ) values changed in steps from one layer to another, as it will be shown below. We tested a variety of conductivity distributions (further called “ σ -distributions”) across the layers, but within the scope of this work, we present only a few of the most relevant ones. As for the electrode names used here: the “hot” electrode is the mid electrode connected to a high-voltage (HV) source; the “grounded” electrode is electrically grounded and linked to the “hot” electrode by a switch between them; the “floating” electrode is neither connected to the HV source, nor grounded.

We used two σ -distributions of the opposite nature, named for this purpose A and B. (The names used for these distributions are not so self-explanatory. They were internally used over the course of this work, but we retain them in this paper for consistency reasons.) In the distribution A, σ is distributed such that the layers next to the electrodes are assigned $\sigma_1 = \sigma_{\max}$ value, while the layer in the center is assigned $\sigma_8 = \sigma_{\min}$. Thus, the σ -distribution is symmetrical around the central layer. In this case, $\sigma_{\max} = 10^{-2}$ S/m, and $\sigma_{\min} = 10^{-10}$ S/m. For 1 V-voltage between the electrodes, the field values for each layer of the lower line are plotted in Fig. 6 with respect to the *homogeneous* case (of a single, lossless slab). (The results for the upper line are omitted as they are always lower or equal to those in the lower line.) The field of the distribution A is lower than that of the *homogeneous* distribution everywhere except in the layers next to the electrodes, where it sharply rises, which is undesirable since the field enhancement is the highest by the hot electrode anyway.

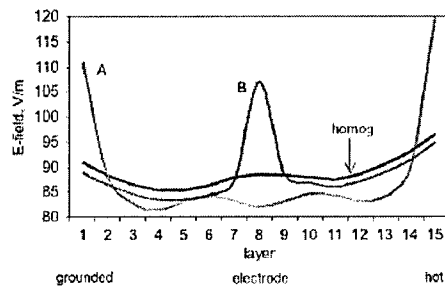


Figure 6. E-field in the lower line (transient) in Fig. 2. We see that all three curves are bundled around the same values, except for a few

For case B ($\sigma_1 = \sigma_{\min}$, $\sigma_8 = \sigma_{\max}$), the field in the transient regime is moderately lower than in the *homogeneous* case everywhere except in the central layer where it has a spike. However, since breakdown can occur in the electrostatic regime just as in the transient regime, we now turn to the situation in the electrostatic regime for these three distributions, which is shown in Fig. 2.

points near the electrodes, and in the center. That was also the case for the other distributions tested (not shown here) and we can generally state that the distribution of the field in the electrostatic regime is quite insensitive to changes in σ -distribution. Attempts to optimize the field values based on the electrostatic regime resulted just in minor differences, which is why in the rest of the discussion we will focus on the improvements in the transient regime.

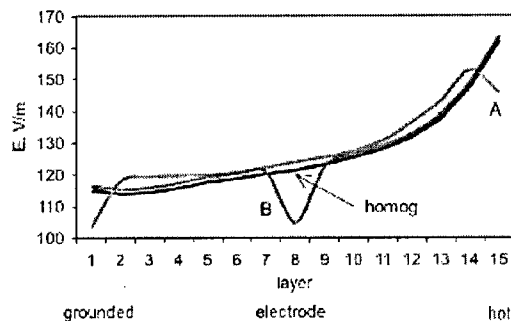


Figure 7. E-field produced by three models in the lower line in electrostatic mode.

These were possible by adjusting the form of the σ -distribution function, and σ_{\max} and σ_{\min} values. Figure 8 shows the most significant of these attempts. The first attempt of optimization of the design, *opt1*, is based on good properties of models A and B. It keeps the same σ_{\max} and σ_{\min} , but applies a form of σ -function in which σ for the inner layers (3 - 13) is based on model A, while σ for the outer layers (1, 2, 14, 15) was based on model B. This brought a notable improvement

over the earlier cases since the field is lower than in the homogeneous case for the most layers, and the field values in the outermost layers are also considerably lower comparing to the values before.

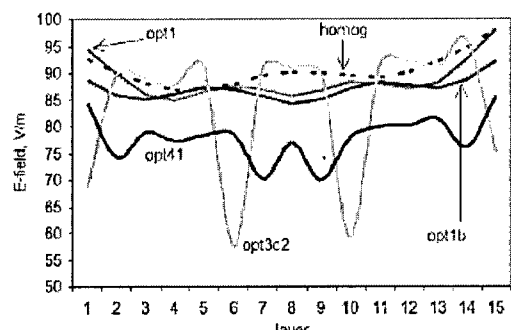


Figure 8. E-field in the transient regime after adjustment of conductivity distribution, and values.

The overall fundamental limitations in using a folded Blumlein transmission line have been identified and summarized.⁵

⁵ M. Joler, C.G. Christodoulou, and E. Schamiloglu, "Limitations to Compacting a Parallel-Plate Blumlein Pulse-Forming Line," accepted and to appear in *International Journal of RF and Microwave Computer-Aided Engineering* (2007).

Liquid Breakdown Studies in Support of Task 1

This research was led by Old Dominion University and is included in their portion of this report.

High Dielectric Constant Ceramics for Use in Blumlein Transmission Lines

Although the folded Blumlein pulser configuration described thus far is compact, it is widely recognized that high energy density ceramic dielectrics can further decrease the volume of such pulser systems and this is what motivates our interest in breakdown in solids. The particular aspect of breakdown in solids that is of interest is a study of breakdown in high dielectric constant ceramics with spatially-varying permittivity (leading to a graded resistivity). High dielectric constant ceramics are being developed for a wide variety of applications in electrical engineering, including as a dielectric for high energy density capacitors.

The energy density γ (in J/m^3) of a ceramic under the influence of an applied electric field is given by

$$\gamma = \epsilon_0 \epsilon_r E^2/2 \quad (2)$$

where ϵ_0 is the permittivity of free space, ϵ_r is the dielectric constant of the ceramic, and E is the applied electric field strength. Typical candidate materials that are being studied in this regard are TiO_2 and $BaTiO_3$.

The development of high dielectric constant ceramics is led by the ceramists, who are concerned with the microstructure and processing techniques used in fabricating samples. Unfortunately, earlier attempts at utilizing nanocrystalline ceramics proved challenging, since the ceramists' ability to reproducibly sinter large quantities of reasonably-sized samples was limited.

We therefore shifted our attention to working with epoxy compounds that were impregnated with nanocrystalline powders. This was a collaborative effort with TPL Inc. (Albuquerque, NM). This ceramic/epoxy composite material which has a high dielectric constant is proprietary in which the nature cannot be disclosed (mystery material).

Precision ball bearings were used as the electrodes to help minimize electrical field enhancement that would create surface flashover. One part consists of 16 samples with the electrodes attached to the mystery materials. When testing, the material would be submerged in high voltage dielectric oil to prevent arcing between the bearings since the bearing are close together and voltages would reach in the realm of 80 kV. There is a gap between the electrodes where the thickness is calculated through measurements. When the ceramic/epoxy composite material was being made, the ball bearings were temporarily glued to a fixture to create the gap between the precision ball bearings. Pictures of the mystery material can be viewed below (part – BB#8) in Figure 8.

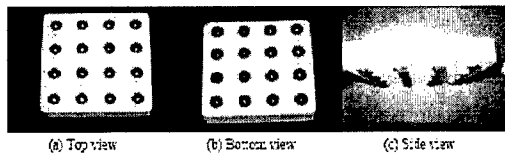


Figure 8. Photograph of precision ball bearings impregnated in the epoxy matrix.

In characterizing the electrical breakdown strength of the mystery material, there were many tests that could have been performed. Due to the limited number of samples, the types of tests to be performed depend on the desired future application of the material. Parts – BB#3, BB#4, and BB #6 underwent a ramp test. Test data can be viewed below. The ramp test was at 20 kV/s until the material broke down.

Tables 1-3 summarize the test data for three samples. With the data combined considering the different thickness between the precision ball bearings (gap containing the mystery material), it was calculated that the average electrical field breakdown was 6.47 kV/mil with a deviation of 0.36 kV/mil or 2.55 MV/cm with a deviation of 0.14 MV/cm.

Sample #	kV/mil	MV/cm	Thickness (mils)	V (kV)
1	5.91	2.33	11.5	67.99
2	6.02	2.37	11.5	69.26
3	6.33	2.49	12	75.94
4	6.40	2.52	12.5	80.02
5	6.42	2.53	13	83.48
6	6.59	2.60	12	79.11
7	6.61	2.60	12	79.34
8	6.70	2.64	13	87.10
9	6.75	2.66	10	67.49
10	6.89	2.71	12	82.67

Table 1. Sample data for BB#3. Using Weibull statistics, it was calculated that the average breakdown voltage was approximately 74.24 kV and the standard deviation was approximately 14.27 kV.

Sample #	kV/mil	MV/cm	Thickness (mils)	V (kV)
1	6.07	2.39	11.5	69.78
2	6.20	2.44	12.5	77.52
3	6.23	2.45	12	74.73
4	6.45	2.54	12	77.42
5	6.57	2.59	12	78.88
6	6.76	2.66	13	87.90
7	7.29	2.87	12	87.42

Table 2. Sample data for part – BB#6. Using Weibull statistics, it was calculated that the average breakdown voltage was approximately 76.10 kV and the standard deviation was approximately 14.60 kV.

Sample #	kV/mil	MV/cm	Thickness (mils)	V (kV)
1	6.07	2.39	5.5	33.39
2	6.09	2.40	5.5	33.47
3	6.17	2.43	6	37.01
4	6.43	2.53	5.5	35.36
5	6.84	2.69	6	41.04
6	7.08	2.79	6.5	46.04

Table 3. Sample data for part – BB#4. Using Weibull statistics, it was calculated that the average breakdown voltage was approximately 38.00 kV and the standard deviation was approximately 7.30 kV.

The key result from testing this mystery material is that, just with other dielectrics tested (such as Mylar), the pulsed power breakdown electric field strength is lower than the quasi-DC breakdown electric field strength. This surprising result has yet to be fully understood. Continued efforts in this direction would be useful.

UNM PERSONNEL

(June 2005 – November 2006)

ECE Faculty

Dr. Edl Schamiloglu (consortium PI), Professor

Dr. Christos Christodoulou (UNM Co-PI), Professor and Chair

ECE Research Faculty

Dr. John Gaudet (0.5 FTE)

Dr. Mikhail Fuks (0.5 FTE)

Dr. Jerald Buchenauer (0.5 FTE)

ECE Staff

Mr. Ralph L. Terry, Laboratory Supervisor (0.5 FTE)

Graduate Students

Miroslav Joler – Ph.D. – Design of High Power Blumlein Transmission Lines (graduated)

Zhaoxian Zhou – Ph.D. – Multiresolution Basis Functions for Transient Field Calculations
Using the Time Domain Integral Equation Method (graduated)

Jinhui Chen – Ph.D. – Electromagnetic modeling of transient breakdown phenomena in
liquids and gases (graduated)

Kelly Hahn – M.S. – HPM generation using Disk Cathode (graduated)

Paul Castro – M.S. – TiO₂-impregnated epoxy for use in compact transmission lines (will
graduate August 2007)

Marvin Roybal – M.S. – Low impedance Marx for relativistic magnetrons (will graduate
August 2007)

Andrey Andreev – Ph.D. – Relativistic magnetron/ubitron with transparent cathode (will
graduate summer 2007)

Sarita Prasad – Ph.D. – Relativistic magnetron with transparent cathode – rapid rise (will
graduate Dec. 2007)

Undergraduate Students

Michael Abney – phase locking of magnetrons (graduated).

UNM PUBLICATIONS

(Since August 2006)

1. Books

a) J. Benford, J. Swegle and E. Schamiloglu, *High Power Microwaves, 2nd Ed.* (Taylor and Francis, New York, NY, February 2007).

2. Journal Papers

a) H. Bosman, M. Fuks, S. Prasad, and E. Schamiloglu, "Improvement of the Output Characteristics of Magnetrons Using the Transparent Cathode," *IEEE Trans. Plasma Sci.* **34**, 606-619 (2006).

b) M. Fuks, N. F. Kovalev, A. Andreev, and E. Schamiloglu, "Mode Conversion in a Magnetron with Axial Extraction of Radiation," *IEEE Trans. Plasma Sci.* **34**, 620-626 (2006).

c) S. Xiao, J. F. Kolb, M. A. Malik, X. Lu, M. Laroussi, R. P. Joshi, E. Schamiloglu, and K. H. Schoenbach, "Electrical Breakdown and Dielectric Recovery of Propylene Carbonate," *IEEE Trans. Plasma Sci.* **34**, 1653-1661 (2006).

d) G. Zhao, R. P. Joshi, V. K. Lakdawala, E. Schamiloglu, and H. Hjalmarson, "TiO₂ Breakdown Under Pulsed Conditions," *J. Appl. Phys.* **101**, 026110-1-3 (2007).

e) M. Joler, C.G. Christodoulou, and E. Schamiloglu, "Limitations to Compacting a Parallel-Plate Blumlein Pulse-Forming Line," accepted and to appear in *International Journal of RF and Microwave Computer-Aided Engineering* (2007).

3. Papers in Conference Proceedings

a) E. Schamiloglu, M. Fuks, H. Bosman, S. Prasad, and A. Andreev, "High-Power Magnetron and Ubitron Powered by a Transparent Cathode," to appear in *Proceedings BEAMS 2006*, (Oxford, UK, July 2006).

b) M. Fuks, A. Andreev, H. Bosman, S. Prasad, and E. Schamiloglu, "Prospective Applications of the Transparent Cathode in Crossed-Field Microwave Oscillators," *Papers of Joint Technical Meeting on Plasma Science and Technology and Pulsed Power Technology, IEE Japan* (Kauai, Hawaii, 7-9 August 2006), p. 61-66.

c) H. Bosman, S. Prasad, M. Fuks, and E. Schamiloglu, "Improved Performance of Magnetrons using the Transparent Cathode," *Proceedings 14th Symposium on High Current Electronics*, (Tomsk, Russia, 10-15 September 2006), p. 346-351.

d) A. S. Shlapakovski, S. N. Artemenko, V. A. Avgustinovich, A. I. Mashchenko, V. M. Matvienko, V. Yu. Mityushkina, I. I. Vintizenko, W. Jiang, and E. Schamiloglu, "Status of the Development of X-Band Antenna-Amplifier: Design, Simulations, and Prototype Experiments," *Proceedings 14th Symposium on High Current Electronics*, (Tomsk, Russia, 10-15 September 2006), p. 359-362.

e) A.S. Shlapakovski, W. Jiang, and E. Schamiloglu, "Numerical Simulations of an X-

Band Antenna Amplifier Device,” *Proceedings 14th Symposium on High Current Electronics* (Tomsk, Russia, 10-15 September 2006), p. 417-420.

d) E. Schamiloglu, M. Fuks, H. Bosman, S. Prasad, and A. Andreev, “High-Power Magnetrons and Ubitrons Driven by Transparent Cathodes,” *Proceedings of the First Euro-Asian Pulsed Power Conference*, (Chengdu, China, 18-22 September 2006), p. ThI-05-1-6.

4. Abstracts

a) S. Prasad, H. Bosman, M. Fuks, and E. Schamiloglu, “Limitation of Leakage Current in the A6 Relativistic Magnetron,” *IEEE International Conference on Plasma Science* (Traverse City, MI, June 2006).

b) M. Roybal, M. Abney, S. Prasad, M. Fuks, C.J. Buchenauer, K. Prestwich, J. Gaudet, and E. Schamiloglu, “Design and Optimization of a Low-Impedance Pulsed Power Marx Generator to Drive a Relativistic X-band Magnetron,” *IEEE International Conference on Plasma Science* (Traverse City, MI, June 2006).

c) A.D. Andreev and E. Schamiloglu, “Measurement of I-V Characteristic of Shortpulse (10-15 ns) Electron Beam,” *IEEE International Conference on Plasma Science* (Traverse City, MI, June 2006).

d) J.T. Fleming, P. Mardahl, L. Bowers, H. Bosman, S. Prasad, M. Fuks and E. Schamiloglu, “Three Dimensional PIC Simulations of the Transparent and Eggbeater Cathodes in the Michigan Relativistic Magnetron,” *IEEE International Conference on Plasma Science* (Traverse City, MI, June 2006).

e) S. Prasad, H. Bosman, M. Fuks, and E. Schamiloglu, “Efficiency Enhancement in A6 Magnetron with Transparent Cathode,” *IEEE International Conference on Plasma Science* (Traverse City, MI, June 2006).

f) A.S. Shlapakovski, S.N. Artemenko, V.M. Matvienko, I. I. Vintzenko, W. Jiang, and E. Schamiloglu, “Status of the Development of X-band Antenna-amplifier: Design, Simulations, and Prototype Experiments,” *IEEE International Conference on Plasma Science* (Traverse City, MI, June 2006).

UNM RECOGNITION

- 1) Edl Schamiloglu elected EMP Fellow, Summa Foundation.
- 2) Andrey Andreev, Sigma Xi outstanding graduate student award.

UNM - NEW DISCOVERIES, INVENTIONS, PATENTS

1. Patent Disclosure: M.I. Fuks, E. Schamiloglu, H. Bosman, and S. Prasad, "An Eggbeater Transparent Cathode for Magnetrons and Ubitrons and Related Methods of Generating High Power Microwaves," UNM-787, provisional patent filed August 25, 2006.

Final Report

on the project

Basic Research Leading to Compact, Portable Pulsed Power

Subcontract to Old Dominion University:

ODU – LIQUID BREAKDOWN AND ENERGY STORAGE

June 1, 2001 – November 30, 2006

submitted to

E. Schamiloglu, P.I.

Department of Electrical and Computer Engineering
University of New Mexico
Albuquerque, NM 87131

by

Karl H. Schoenbach

Frank Reidy Research Center for Bioelectrics
Old Dominion University
830 Southampton Avenue, Suite 5100, Norfolk, VA 23510
Tel. 757-683-2421
FAX: 757-314-2397
e-mail: Schoenbach@ece.odu.edu

ODU INTRODUCTION

The research work at Old Dominion University has focused on experimental and modeling studies on breakdown of electrical discharges in polar liquids, and their application for energy storage and as closing switches in compact pulsed power systems. The liquids studied were water and propylene carbonate. While water is widely used as an energy storage medium in fast pulse forming networks with the advantages of low cost, high availability, and ease of handling, its freezing temperature of 0°C prohibits its use in lower temperature environments. An alternative candidate is propylene carbonate (C₄H₆O₃). It is a polar liquid and has a dielectric constant of 65. Its freezing temperature is -55°C, which is more suitable for lower temperature applications, for example, as energy storage and switch medium in airborne systems, which operate at high altitude.

ODU - LIST OF ACHIEVEMENTS

In our work, which was performed in collaboration with the research group at the University of New Mexico (Dr. Schamiloglu), and also with our colleagues from the sister MURI consortium at Texas Tech University in Lubbock, TX, we:

- Determined the dielectric strength of water and propylene carbonate depending on pulse duration, covering the range from microseconds to ten's of nanoseconds. The results showed that the dielectric strength in a pin-plane electrode geometry depends on polarity. Whereas for negative polarity of the pin, the results confirm Martin's empirical equation, but for positive polarity, they are higher than predicted. The dielectric strength of water, which increases inversely with pulse duration, reaches 1.8 MV/cm and 1.5 MV/cm for negative and positive pin polarity for 50 ns pulses. It was higher (2.2 MV/cm) for propylene carbonate under the same conditions.
- Explored the breakdown mechanism in polar liquids in response to a submicrosecond (~100–200 ns) voltage pulse. It was shown, through simulations, that breakdown is initiated by field emission at the interface of preexisting micro-bubbles. Impact ionization within the microbubble's gas then contributes to plasma development, with cathode injection having a delayed and secondary role. The models developed adequately explained experimental observations of pre-breakdown current fluctuations, streamer propagation and branching, as well as disparities in hold-off voltage and breakdown initiation times between the anode and the cathode polarities. It was demonstrated that polarity effects basically arise from the large mobility difference between electrons and ions.
- Studied the breakdown mechanism experimentally by using ultrashort optical and electrical diagnostics. In particular, by using interferometric methods, we determined the spatial and temporal development of the precursors of the conducting plasma, and to determine the absolute values of the electric field by means of the Kerr effect.
- Studied the recovery phase after breakdown in water. Whereas the physics of the breakdown determines the important closing switch parameters such as breakdown

voltage, current rise and plasma development, recovery is important for any system that operates in a repetition rate mode. Experiments using pulse-probe methods and Schlieren diagnostics allowed us to follow the development of the disturbance caused by the breakdown over a time of more than milliseconds. After breakdown, the expanding plasma column generates shockwaves first and later, a vapor bubble which expands for approximately 200 μ s and then decays with a time constant of 1 ms. The bubble decay time determines the dielectric recovery of the switch, as has been shown with pulse-probe experiments.

- Studied the recovery phase after breakdown in propylene carbonate. The recovery of propylene carbonate was found to be similar to that of water, with plasma decay, shock wave emission, and vapor bubble formation, except for the very last phase, which is determined by chemical reactions: the generation and decay of polypropylene polymers. This restricts the time for dielectric recovery of propylene carbonate switches to values of more than 10 ms.

Whereas these achievements have been reported in earlier annual reports, our efforts during the past 15 months have focused on developing triggerable, compact pulsed power systems which utilize the advantages of liquids as energy storage and switch medium.

High repetition-rate, compact, nanosecond pulse generator

We have built and tested a pulse generator that provides a 10 ns duration, 2 ns risetime, up to 35 kV pulse amplitude across a matched load. The current rise obtained reaches values of almost 2 kA/ns. In addition, the pulse generator allows us to operate at repetition rates exceeding 100 Hz. This has been achieved by using water switches in a flow-through configuration. We were able to reach a repetition rate of up to 400 Hz, limited only by the power supply. Earlier studies using the same concept have shown that it is possible to exceed 1 kHz repetition rates.

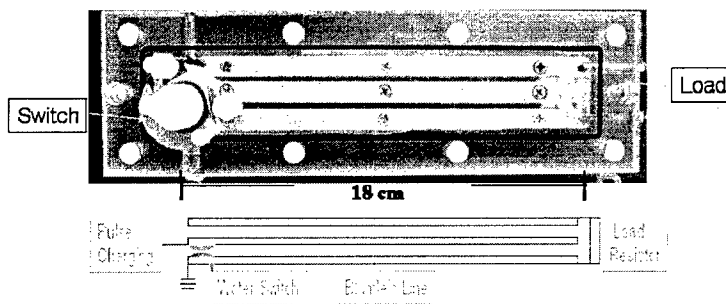
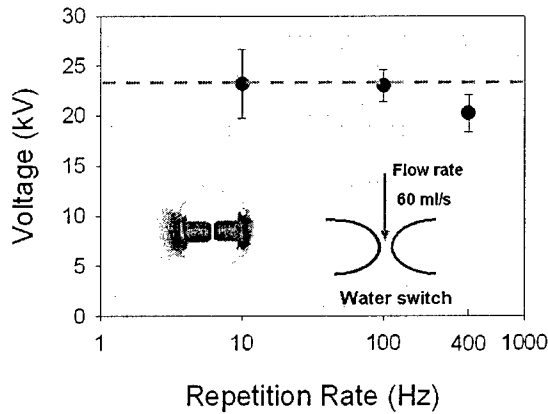


Fig. 1 Photograph and cross-section of the all-water pulse generator

By using flowing, deionized water with its high dielectric constant (81) as dielectric between the parallel lines of the Blumlein PFL, we have the additional benefit of considerable size reduction in the PFL and thermal control of the dielectric. The "all water" pulse generator occupies a volume of only 25 cm by 5 cm by 7 cm, not counting the charging circuit and the hydraulic system. It generates peak powers of more than 100 MW at average powers of half a kW when operated at 35 kV.



rate.

Fig. 2 Breakdown voltage versus repetition rate (inserts: electrodes and schematics of water flow)

- Transverse flow allows repetitive operation at 400 Hz at an average power of 160 W.
- At 400 Hz, the average breakdown voltage decreases by only 13% as compared to the breakdown voltage at 10 Hz.
- Higher repetition rate (higher average power) is possible with increased flow

Electrical Triggering of Water Switches

Triggering breakdown in liquid switches has been achieved with lasers and also with field distortion electrodes. The concepts of laser triggering are straightforward: they are based either on the generation of a preionized channel between the electrodes, or the vaporization of the liquid in the point of the laser beam. For field distortion, the trigger electrode is placed close to the ground electrode along an equal-potential surface. When the trigger electrode reaches high voltage potential, the voltage between the trigger electrode and the electrode with the same polarity decreases, and that of the opposite electrode increases. The breakdown of the overstressed second gap forces the full switch potential to appear across the first gap resulting in complete closing of the switch.

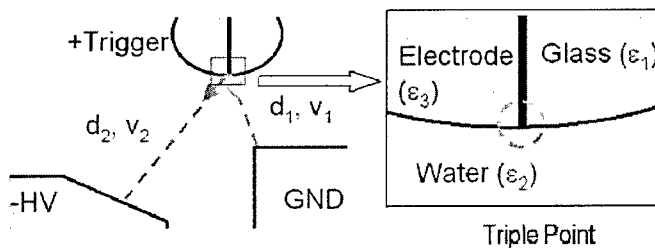


Fig. 3. Concept of a water switch trigatron

We have focused on a different triggering approach that relies on electrically generated positive streamers. The trigatron water switch, which utilizes a trigger electrode with a triple point, has been shown to trigger the water switch with a lower trigger voltage than the field distortion trigger concept. It is due to the initiation of the trigger streamer from a triple point, where the electric field can reach extremely high values, even at moderate voltages. From the triple point, positive streamers send out two filaments that bridge the gaps to the high voltage electrode and ground electrode, providing a conductive path between the electrodes.

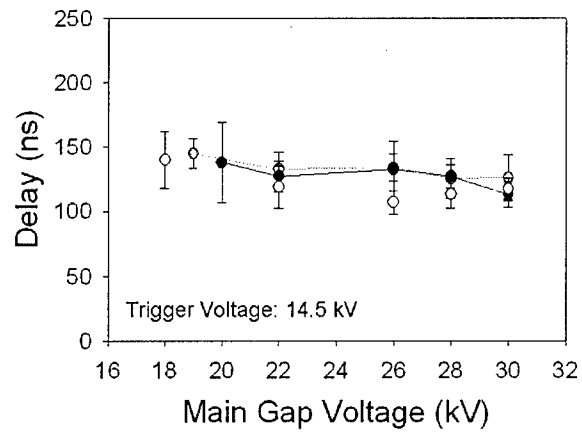
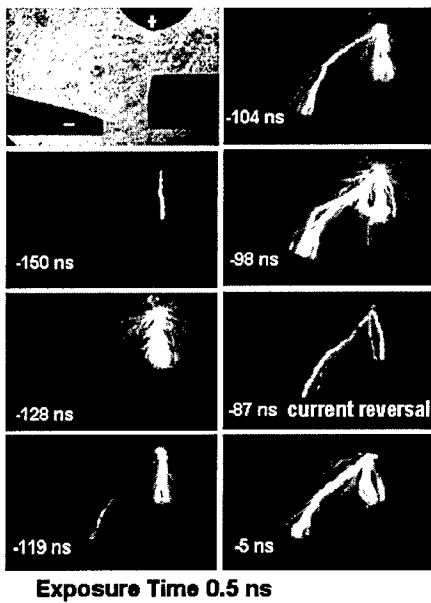


Fig. 4a (left) Streamer development in the water switch trigatron (the first photograph in this series shows the electrode geometry). 4b (above) Delay (and jitter) of trigatron switch versus switch voltage.

A manuscript which discusses the concept and the results of our water switch trigatron research is under preparation.

ODU PUBLICATIONS

(Since August 2006)

Publications in Refereed Journals

- a) Y. Sun, S. Xiao, J. A. White, J. F. Kolb, and K. H. Schoenbach, "Compact, Nanosecond, High Repetition-Rate, Pulse Generator for Bioelectric Studies," submitted to IEEE Trans. Dielectrics and Electrical Insulation
- b) J. Qian, R. P. Joshi, K. H. Schoenbach, J. R. Woodworth and G. Sarkisov, "Model Analysis of Self- and Laser-Triggered Electrical Breakdown of Liquid Water for Pulsed Power Applications," IEEE Trans. Plasma Science 34, 1680-1691 (2006).
- c) S. Xiao, J. Kolb, M. A. Malik, X. Lu, M. Laroussi, R. P. Joshi, K. H. Schoenbach, "Electrical Breakdown and Dielectric Recovery of Polar Liquids," IEEE Trans. Plasma Science 34, 1653-1661 (2006).
- d) J. Qian, R. P. Joshi, E. Schamiloglu, J. Gaudet, J. R. Woodworth, and J. Lehr, "Analysis of the Polarity Effects in the Electrical Breakdown of Liquids," J. Phys. D 39, 359 (2006).
- e) Juergen F. Kolb, Susumu Kono, and Karl H. Schoenbach, "Nanosecond Pulsed Electric Field Generators for the Study of Subcellular Effects," Bioelectromagnetics J. 27, 172-187 (2006).

Publications in Conference Proceedings

- a) E. Schamiloglu, K. H. Schoenbach, R. Vidmar, R. P. Joshi, M. Laroussi, J. F. Kolb, and S. Tyo, "Compact, Portable Pulsed Power – Lessons Learned and Quo Vadis," to appear in the Conf. Record of the 2006 IEEE Power Modulator Conference, Washington DC, May 14-18, 2006.
- b) Tammo Heeren, Juergen F. Kolb, Shu Xiao, Karl H. Schoenbach, and Hidenori Akiyama, "Pulsed Power Generators and Delivery Devices for Bioelectrical Applications," to appear in the Conf. Record of the 2006 IEEE Power Modulator Conference, Washington, D.C. May 14-18, 2006.
- c) Y. Sun, S. Xiao, J. F. Kolb, K. H. Schoenbach, "A Nanosecond, High Repetition-Rate, All Water Pulse Generator," to appear in the Conf. Record of the 2006 IEEE Power Modulator Conference, Washington, D.C. May 14-18, 2006.
- d) S. Xiao, Y. Sun, J. Kolb, U. Pliquet, T. Heeren, H. Akiyama, and K. H. Schoenbach, "Electrically Triggered Water Switches," to appear in the Conf. Record of the 2006 IEEE Power Modulator Conference, Washington, D.C. May 14-18, 2006.

Final Report

21 Dec 2006

**IMPROVEMENTS TO COMPONENTS FOR USE IN COMPACT PULSED
POWER SYSTEMS**

By: ROBERT J VIDMAR

Prepared for:

Professor Edl Schamiloglu, MURI Principal Investigator
University of New Mexico
ECE Department - Pulsed Power, Beams and Microwaves Laboratory
Albuquerque, NM 87131-0001

CONTRACT NUMBER: UNM Subaward 3-19531-7820
Based on AFOSR F49620-01-1-0354

Approved for Public Release: Unclassified with Distribution Unlimited

University of Nevada, Reno
1664 North Virginia Street
Reno, Nevada 89557-0240 USA

UNR ABSTRACT

Research on the overall effort has been on exponential transmission lines with high-impedance ratios and high-pressure liquid cooling of active and passive electronic components. The most recent work addresses transmission-line design and practical RF line termination to permit pulsed operation with nanosecond or better rise time. A geometrical algorithm is used to provide a line shape that incorporates an exponential variation in line impedance and maintains a constant phase front throughout the transmission line. This modification permits line operation with impedance ratios exceeding 10 with a test transmission line operating with an impedance ratio of 100. Line termination with a RF load distributed along the output interface is critical to observing ideal voltage step-down performance. Driving the low-impedance end of the line requires a uniform distribution of feed points along the low-impedance end of the line. Practical realization of the necessary hardware is difficult.

UNR INTRODUCTION

Transmission-line theory has been developed and applied to many applications. A subset of transmission line theory that deals with lines with nonuniform properties has received significant attention but some devices such as an exponential transmission line remain theoretical¹ without discussion on practical limits to line performance. A basic property of an exponential line is its performance as an ideal high-pass transformer. An early investigation by Johnson² provides clear insight on exponential line operation such as voltage step-up and impedance transformation but provides no insight on practical limits of performance. Latter investigators provide analytic expressions of circuit parameters including two-port S parameters³⁻⁵. Agreement between theory and experiment is very good for short transmission lines with impedance ratios of less than thirty⁶. Such devices are relatively compact and have been used extensively as impedance matching devices for couplers. Although the S-parameters provide a complete theoretical analysis for small impedance ratios, they provide no answers to the practical limits experienced when constructing an exponential line with impedance transformations ratios greater than thirty.

Basic theory for an exponential line has a sound theoretical footing and Vidmar and Faretto⁷ provide an explanation and experimental findings that suggest the limitations to exponential lines with high impedance ratios can be overcome with a modified exponential shape. A major constraint on the exponential-line shape is that all rays in a propagating wavefront propagate at the same speed and the phase is uniform along a curved wavefront. Traditional theory maintains a planar wavefront resulting in significant interference for lines with impedance ratios greater than thirty. Zucker *et al*⁸ demonstrated a long exponential line with the thickness of the line above the ground plane tapered. That taper over part of the line in conjunction with a gentle increase of line width of a different part of the line resulted in an overall impedance ratio of 200. The Zucker line could be made more compact by incorporating the modified exponential shape and applying it along the entire transmission-line length.

Exponential lines provide a means of transforming a low-voltage high-current pulse into a high-impedance high-voltage pulse. Several lines can be combined in a parallel-series configuration using two-port network theory. One implementation is to combine several lines with the low-impedance sides driven in parallel and the high-impedance ends arranged in series. This topology provides a method of combining high-voltage pulses to obtain a very high-voltage pulse. Research on a exponential line with an impedance ratio of 100 has provided a means of achieving compact lines with high impedance ratios.

UNR - LIST OF ACHIEVEMENTS

A. Exponential Transmission Line Modeling

The exponential line model⁷ was used to design an exponential line with an impedance ratio of 100. A ray tracing algorithm was developed to maintain the phase of a propagating wavefront and to adjust the arc length of the wavefront to increase in an exponential manner. The resulting algorithm was programmed to generate a taper that approximates an exponential line. The exponential line has a high-impedance of 50 Ω and a low-impedance of 500 m Ω . The line was fabricated from a thick copper sheet ground plane and 1-mm thick Teflon as a dielectric layer between the upper transmission line surface and the ground plane. The geometry was fine tuned for minimum backscatter from the high-impedance (50 Ω) end using the S_{11} parameter of a vector network analyzer. Measurements were conducted with continuous signals at discrete frequencies above the high-pass cutoff frequency and for a 2-ns duration pulse. These experiments yielded an approximate voltage step-down ratio of 10.

B. RF Power Termination

The low-impedance end of the line was terminated with multiple resistors closely spaced. The number of resistors and their value were computed based on multiple resistors in parallel. Industrial composition resistors were initially used to terminate the line. They provided some results but the resistors failed to function properly at high frequency due to excessive reactance. RF resistors were used but they were not rated for GHz operation. The results presented by Vidmar and Faretto⁷ used these resistors and strongly suggested that the termination resistors need to have a multi-GHz rating for proper termination. RF resistors were investigated and vendors identified. A quantity of 40- Ω RF resistors were custom ordered from Mini-Systems Inc. Their series WAMT 1AT-40R00G-T resistors are rated for 20 GHz operation with 2% tolerance and are tinned for solder application. These resistors have a length of 40 mils or approximately 1 mm.

A technique was developed to solder these resistors to a small copper ground plane test plate. A pre-warming fixture in conjunction with a 300 W soldering iron was necessary to melt solder. Soldering resistors involved tinning the test plate, applying a rosin flux, hot-air drying the rosin till it was tacky, picking up the resistor with a vacuum pick-up tool, and positioning it on the tacky rosin. With the resistor in place and the plate pre-warmed, it was possible to apply heat from the 300-W soldering iron approximately 1 to 2 inches from the resistor. After a few seconds of heating, a melting wave front appears and propagates to the resistor. When the wavefront hits the resistor, capillary attraction sucks solder to the resistor, fixing it in place. Application of this technique on the massive transmission line failed, because differential thermal expansion of the copper plate resulted in significant buckling. A large Teflon sheet that covers the copper ground plane and serves as the dielectric layer in the transmission line is also heated resulting in additional buckling at the Teflon-to-copper interface. The small resistors were attracted to the small gaps between the copper ground

plane and the Teflon sheet via capillary attraction of the liquid rosin and solder. The resistors moved out of position with some of them appearing to get sucked under the Teflon.

The soldering approach is very difficult because of buckling of the copper sheet and the Teflon. Fixturing individual resistors in place and soldering were considered, but that would not alleviate buckling and the prospect of permanent mechanical distortion of the ground plane and Teflon sheet. Uniform heating of the entire end of the transmission line in a large oven would alleviate buckling but the infrastructure to do so was not available. An approach using conductive epoxy alleviates the buckling and distortion issue noted but requires a special surface treatment of the ends of the resistors for proper RF operation. Lead time to procure appropriate resistors was approximately three months and the research effort terminated before a solution to this problem could be implemented.

UNR - SUMMARY OF RESULTS

The major research results are the following:

- Quantify Theoretical Limits of Exponential Lines with High Impedance Ratios.
- Quantify Performance of High-Impedance Transmission Line.
- Utilization of RF Chip Termination Resistors.

A. Limitations in Implementation of Exponential Line Theory

The ray propagation model provides a refinement in the mechanical design of an exponential line with a high-impedance ratio. This refinement provides a method of designing a compact transmission line by combining a dielectric taper as well as expanding the line width at the low-impedance end of the line to achieve maximum impedance ratio with minimum length. The limitation on minimum line length and maximum line impedance ratio is driven by phase variations at the low-impedance end of the line and material properties. At the high-impedance end of the line dielectric breakdown voltage and width of the current conductor provides a practical limit of approximately one thousand ohms. At the low-impedance end of the line, the line is wide and the dielectric can be thinner because the voltage is lower. The thickness of dielectric can be tapered down by a factor of the square root of the impedance ratio. A typical value of fifty milliohms may be achieved at the low-impedance end of the line. A total impedance ratio of one thousand should be possible with a very hard to achieve upper limit of approximately ten thousand. The experiments conducted provide a practical input on the overall feasibility of constructing compact exponential lines with high-impedance ratios.

B. Results from an Exponential Line with a 100-to-1 Impedance Ratio

The investigation of a 100-to-1 impedance ratio exponential line demonstrates the feasibility of an approach to maintain coherent phase fronts at the wide low-impedance end of an exponential line. Tuning the line in real time for minimum reflections using a network analyzer set for S_{11} was very effective. When S_{11} is displayed in time-domain mode, small irregularities along the length of the line were easily identified and corrected. The results demonstrated an approximate 10-to-1 voltage step-down ratio in correspondence to theory. Pure resistive termination at the low-impedance end is necessary for proper high-frequency operation and minimization of internal reflections within the line. When driving the line from the low-impedance end, it is important to have nearly ideal components that have a minimum of reactance at the frequencies of interest.

C. Utilization of RF Chip Termination Resistors

The overall experience in working with 1-mm long RF termination resistors is that soldering is a difficult activity and is not well suited to large thick surfaces. If soldering is to be utilized in fixing resistors, a thin copper sheet for a ground plane is preferred to a thick sheet. An alternative approach is to use RF chip resistors specified with an end treatment which is compatible with conductive epoxy adhesives. The latter approach eliminates the thermal expansion issue of buckling associated with direct soldering and provides additional finesse in final placement of resistors.

UNR PERSONNEL

Personnel. The primary personnel on this project has been

- Robert J Vidmar, Principal Investigator

Additional personnel that contributed to the project

- Harold Faretto, Electronics Technician
- Andrew Oxner, Development Technician
- Quinn Sinnott, Undergraduate Student Worker

Interactions. The principal research has been presented at the 15th International Pulsed Power Conference, Monterey, CA 2005. There were several interactions at these conferences with representatives from DoD Laboratories, National Laboratories, private companies, and Universities from around the world.

UNR PUBLICATIONS

Vidmar, R, and H Faretto, "Exponential Transmission Line Design for Impedance Ratios Greater than 10, 15th International Pulsed Power Conference, 13-17 June, paper 10120, Monterey, CA, 13-17 June 2005.

UNR REFERENCES

- [1] G Miano and A Maffucci, *Transmission Lines and Lumped Circuits*, Academic Press, San Diego, CA, pp 271-279, 2001.
- [2] W. C. Johnson, *Transmission Lines and Networks*, McGraw-Hill, New York, pp. 201-208, 1950.
- [3] V. Ramachandran, and K. K. Nair, "Equivalent Circuits of an Exponential Transmission Line", *IRE Trans. on Circuit Theory*, vol. CT-7, pp. 71-74, 1960.
- [4] S. C. Dutta Roy, "Low-Frequency Wide-Band Impedance Matching by Exponential Transmission Lines," *Proc. of the IEE*, vol. 67, pp. 1162-1163, 1979.
- [5] R. J. Vidmar, 14th International Conference on High-Power Particle Beams, BEAMS 2002, June 23-28, 2002, *AIP Conference Proceedings*, vol. 650, pp. 41-44, 2002.
- [6] R. P. Arnold and W. L. Bailey, *Electronic Design*, vol. 22, 136-139 (1974).
- [7] R. Vidmar and H. Faretto, "Exponential Transmission Line Design for Impedance Ratios Greater than 10", *15th International Pulsed Power Conference*, 13-17 June, paper 10120, Monterey, CA, 13-17 June 2005.
- [8] O. S. F. Zucker, D. Giorgi, K. Stuurman, K. Cardwell, P Solone, and M. Bonebright, "Design and Experimental Performance of a Picosecond Rise-Time Adiabatic Transformer with Impedance Ratio of 200:1," *Pulsed Power Conference 1993, Digest of Technical Papers*, pp 297-299, 9th IEEE International, Vol 1, 21-23 June, 1993.